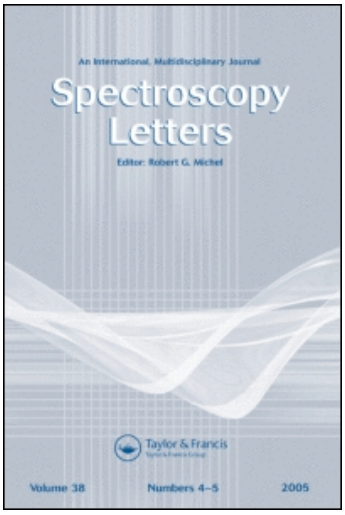

Spectroscopy Letters
Publication details, including instructions for authors and subscription information:
http://www.informaworld.com/smpp/title~content=t713597299

Optical Spectroscopy of Sm^{3+} and Dy^{3+} Doped ZnO Nanocrystals

Yongsheng Liu[a]; Renfu Li[a]; Wenqin Luo[a]; Haomiao Zhu[a]; Xueyuan Chen[a]
[a] Key Laboratory of Optoelectronic Materials Chemistry and Physics, Fujian Institute of Research on the Structure of Matter, Chinese Academy of Sciences, Fuzhou, Fujian, China

Online publication date: 30 July 2010

To cite this Article Liu, Yongsheng , Li, Renfu , Luo, Wenqin , Zhu, Haomiao and Chen, Xueyuan(2010) 'Optical Spectroscopy of Sm^{3+} and Dy^{3+} Doped ZnO Nanocrystals', Spectroscopy Letters, 43: 5, 343 — 349
To link to this Article: DOI: 10.1080/00387010.2010.486717
URL: http://dx.doi.org/10.1080/00387010.2010.486717

Spectroscopy Letters, 43:343–349, 2010

ISSN: 0038-7010 print/1532-2289 online
DOI: 10.1080/00387010.2010.486717

Taylor & Francis
Taylor & Francis Group

Optical Spectroscopy of Sm^{3+} and Dy^{3+} Doped ZnO Nanocrystals

Yongsheng Liu, Renfu Li, Wenqin Luo, Haomiao Zhu, and Xueyuan Chen

Key Laboratory of Optoelectronic Materials Chemistry and Physics, Fujian Institute of Research on the Structure of Matter, Chinese Academy of Sciences, Fuzhou, Fujian, China

ABSTRACT Sm^{3+} and Dy^{3+} ions doped hexagonal wurtzite ZnO nanocrystals were fabricated by a sol-gel method. The obtained ZnO nanocrystals were characterized using the X-ray diffraction, transmission electron microscopy, ultraviolet-visible reflectance spectra, and low-temperature luminescence spectroscopy. Intense and well resolved emission lines for Sm^{3+} and Dy^{3+} ions can be achieved via an energy transfer process from ZnO host to the dopants. It was found that the host sensitized emissions were more efficient than that of direct excitation for Sm^{3+} and Dy^{3+} ions. Moreover, multiple sites of Sm^{3+} and Dy^{3+} ions in ZnO nanocrystals were identified based on the low-temperature photoluminescence spectra.

KEYWORDS energy transfer, lanthanide, multiple sites, photoluminescence, ZnO nanocrystal

INTRODUCTION

Trivalent lanthanide ions (Ln^{3+}) doped nanomaterials are technologically important for the potential applications in optoelectronic devices, flat panel displays and biological labels, which presently have received considerable research interest due to their unique luminescent properties.[1–6] However, because of the parity-forbidden nature of *f-f* transitions of Ln^{3+} ions, the direct excitation for most Ln^{3+} ions is usually inefficient and somewhat restrains them from applications in aforementioned practical fields. To overcome this shortcoming, the host sensitization, namely, the energy transfer (ET) from the excited host to Ln^{3+} ions is desirable in terms of the strong absorptions in the ultraviolet (UV) region especially for most semiconductors. The luminescence of Ln^{3+} ions is thereby expected to be greatly enhanced via an efficient nonradiative ET from the semiconductor host to the dopants. Recently, many significant results for Ln^{3+} ions doped semiconductor nanomaterials have been reported.[4–23] Intense host sensitized emissions of Ln^{3+} ions could be achieved in Ln^{3+} ions doped semiconductor nanomaterials such as TiO_2[4,6,20] and ZnO.[9,11,17,24] Among these materials, ZnO is a well known wide band-gap semiconductor and a prominent candidate to be used as the host materials for the embedding of Ln^{3+} ions due to its outstanding optical and thermal properties. In our recent work, by using a modified sol–gel method, Eu^{3+} ions were successfully incorporated in the ZnO lattices. Multiple sites of Eu^{3+} as well as the host-to-Eu^{3+}

Received 22 July 2009;
accepted 10 October 2009.

Address correspondence to Xueyuan Chen, Key Laboratory of Optoelectronic Materials Chemistry and Physics, Fujian Institute of Research on the Structure of Matter, Chinese Academy of Sciences, Fuzhou, Fujian 350002, China. E-mail: xchen@fjirsm.ac.cn

ET were observed in ZnO:Eu^{3+} nanocrystals.[9,14] Intense near-infrared emission lines with well resolved crystal-field (CF) splittings were also detected for Nd^{3+}- and Tm^{3+}-doped ZnO nanocrystals.[5] Zeng et al. have also observed the host-to-Eu^{3+} ET in ZnO:Eu^{3+} nano-sheet-based hierarchical microspheres fabricated via a hydrothermal strategy,[11] while no similar ET was observed for any other Ln^{3+} ions.[15] Additionally, it should be noted that the majority of attentions in the system of Ln^{3+} doped ZnO were primarily focused on the Eu^{3+} doping, and only broad emission lines of Eu^{3+} could be observed via host sensitization for most cases.[7,24,25] To date, no detailed photoluminescence (PL) properties as well as the host-to-dopants ET process have been reported for Sm^{3+} and Dy^{3+} doped ZnO nanocrystals, which may be beneficial to the understanding of the basic physical and chemical properties of Ln^{3+} ion-doped ZnO nanomaterials.

In this work, we have successfully doped Sm^{3+} and Dy^{3+} into the wurtzite ZnO nanocrystals via a facile sol–gel process, which thus emitted intense and typical emission lines originating from the *f-f* transitions of Sm^{3+} and Dy^{3+} ions. Optical properties including PL excitation, emission spectra and PL dynamics for Sm^{3+}- and Dy^{3+}-doped ZnO nanocrystals were investigated in detail at low temperature.

MATERIALS AND METHODS

The Sm^{3+} and Dy^{3+} ions doped ZnO nanocrystals, with the nominal doping concentrations of 1 at.%, were prepared by employing a modified sol–gel method similar to the report elsewhere.[9] In a typical procedure to the synthesis of Sm^{3+} and Dy^{3+} ion-doped ZnO nanocrystals, 0.01 mol zinc acetate dihydrate (AR) and the required amount of samarium or dysprosium acetate hexahydrate (99.99%) were mixed in a 250 ml round-bottom flask and dried at 120°C for 1 h to remove the adsorbed water. After cooling to room temperature (RT) naturally, 100 mL absolute ethanol was added to the round-bottom flask. The mixture was vigorously stirred with a magnetic stirrer and refluxed at 80°C water bath for 3 h to form a clear precursor solution, and then cooled to 0°C immediately. The addition of 0.025 mol lithium hydroxide monohydrate powder in an ultrasonic bath led to the hydrolysis of the precursor solution and aimed at the charge compensation between Zn^{2+} and Sm^{3+} (or Dy^{3+}) in ZnO nanocrystals. After hydrolyzing at 0°C for 30 min, the ZnO nanocrystals were precipitated by the addition of 300 mL hexane, collected using centrifugation and washed with ethanol several times, and then dried at 60°C for 12 h to afford the as-grown samples. To enhance the crystallinity and luminescence of Sm^{3+} and Dy^{3+} ion-doped ZnO nanocrystals, the as-grown samples were further annealed at 400°C in air for 30 min to yield the final white products.

The precise contents of Sm^{3+} and Dy^{3+} ions were determined to be 1.05 and 1.02 at.% by the Ultima2 ICP optical emission spectrometer, respectively. The morphologies, crystallinity and phase purity of the samples were characterized by a PANalytical X'Pert PRO powder diffractometer and JEOL-2010 transmission electron microscope (TEM). The RT UV-visible diffuse reflectance spectra for Sm^{3+} and Dy^{3+} doped ZnO nanocrystals were recorded on a Perkin-Elmer Lambda 900 UV/vis/NIR spectrometer using $BaSO_4$ as a reference. Emission and excitation spectra were recorded on an Edinburgh Instruments FLS920 spectrofluorimeter equipped with both continuous (450 W) and pulsed xenon lamps. For low temperature measurements, all samples were mounted on a closed cycle cryostat (10–350 K, DE202, Advanced Research Systems). The line intensities and positions of the measured spectra were calibrated according to the FLS920 correction curve and standard mercury lamp.

RESULTS AND DISCUSSION

The crystallinity and phase purity of the samples were investigated by the X-ray diffraction (XRD) and TEM analysis. As shown in Fig. 1b and 1c, the XRD patterns for Sm^{3+} and Dy^{3+} doped ZnO nanocrystals heat-treated at 400°C show peak positions that match well the standard pattern of hexagonal wurtzite ZnO (JCPDS No. 36-1451) and the XRD pattern for pure ZnO nanocrystals (Fig. 1a), indicative of the presence of highly crystalline ZnO nanocrystals without any other impurity phases such as Sm_2O_3 and Dy_2O_3. By virtue of the Debye-Scherrer's formula, the mean sizes for Sm^{3+} and Dy^{3+}-doped ZnO nanocrystals calculated from the diffraction peak (110) are ~14 and 12 nm, respectively. The

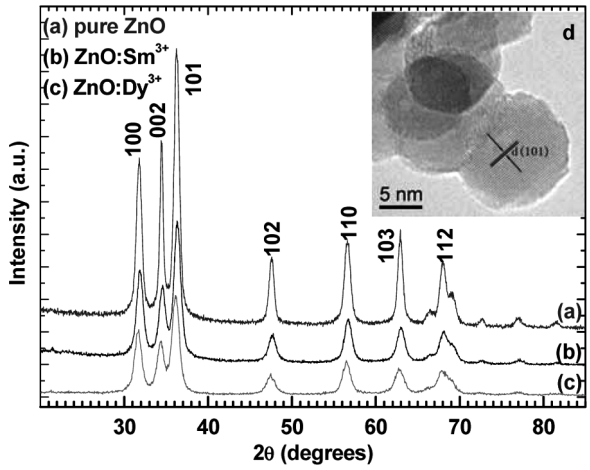

FIGURE 1 XRD patterns for (a) pure ZnO, (b) Sm^{3+}- and (c) Dy^{3+}-doped ZnO nanocrystals, and (d) high resolution TEM image for Sm^{3+}-doped ZnO nanocrystals.

corresponding high-resolution TEM image (Fig. 1d) reveals that the Sm^{3+}-doped ZnO nanocrystals are not ideally spherical with diameters ranging from 10 to 15 nm, which is basically in agreement with the XRD estimates. The crystalline lattice fringes of ZnO nanocrystals are very clear with an observed *d*-spacing of 0.25 nm, which corresponds to the lattice spacing for the (101) planes of hexagonal wurtzite ZnO, further confirming the higher crystallinity of the annealed ZnO nanocrystals. Similar morphology is also observed for Dy^{3+}-doped ZnO nanocrystals.

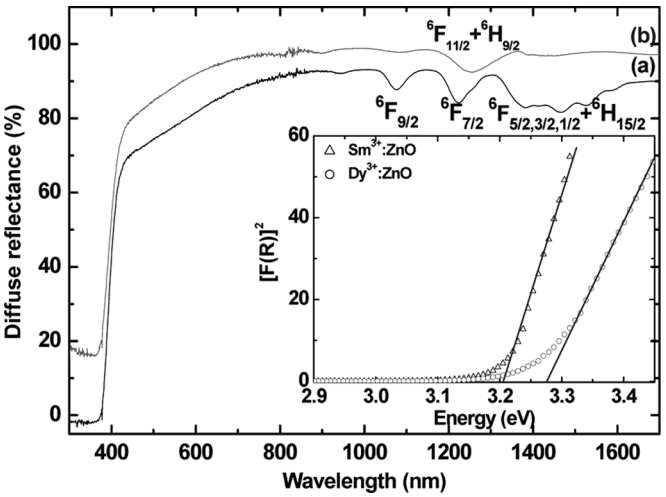

FIGURE 2 The RT diffuse reflectance spectra for Sm^{3+}- (a) and Dy^{3+}- (b) doped ZnO nanocrystals. The inset shows the plot of $[F(R)]^2$ versus photon energy of Sm^{3+}- and Dy^{3+}-doped ZnO nanocrystals, where $F(R) = (1-R)^2/2R$, and R is the reflectance. Band-gap energies of ZnO nanocrystals can be determined by the extrapolation to $[F(R)]^2 = 0$.

The UV/vis diffuse reflectance spectra for Sm^{3+} and Dy^{3+}-doped ZnO nanocrystals were recorded by using $BaSO_4$ plate as a reference. As shown in Fig. 2a and 2b, both samples exhibit a strong absorption onset at ~370 nm, which corresponds to the excitonic $1S_h \rightarrow 1S_e$ transition of ZnO. In addition to the strong absorption of ZnO nanocrystals in the UV region, some characteristic *f-f* absorption peaks of Sm^{3+} and Dy^{3+} can be assigned, which are attributed to the transitions from the ground state of $^6H_{5/2}$ to $^6F_{9/2}$, $^6F_{7/2}$, $^6F_{5/2,3/2,1/2} + {}^6H_{15/2}$ for Sm^{3+} ions (Fig. 2a) and from the ground state of $^6H_{15/2}$ to $^6F_{11/2} + {}^6H_{9/2}$ for Dy^{3+} ions (Fig. 2b), respectively. To derive the band-gap energies (E_g) for Sm^{3+} and Dy^{3+} ion-doped ZnO nanocrystals, $[F(R)]^2$ versus photon energy hv is plotted in the inset of Fig. 2, where $F(R)$ is the Kubelka-Munk function with $F(R) = (1-R)^2/2R$,[26] and R is the observed diffuse reflectance in UV/vis spectra. Adopting the method proposed by Cao et al.,[27] the band-gap energies (E_g) for Sm^{3+}- and Dy^{3+}-doped ZnO nanocrystals are determined to be 3.21 and 3.27 eV (Fig. 2, inset), respectively, by the extrapolation to $[F(R)]^2 = 0$. The slightly larger E_g for Dy^{3+}-doped ZnO nanocrystals compared to that of Sm^{3+}-doped ZnO nanocrystals might be caused by the quantum confinement effect of the smaller nanoparticles.

To study the optical properties of Sm^{3+} ions in ZnO nanocrystals, the PL excitation and emission spectra for Sm^{3+}-doped ZnO nanocrystals were measured at 10 K. As shown in Figure 3a, upon excitation above the ZnO band-gap energy (~370 nm), intense and typical emission lines of Sm^{3+} ions centered at 572.7, 614.9, 658.6 and 722.2 nm are detected at 10 K, which can be assigned to the radiative transitions from $^4G_{5/2}$ to its low-lying multiplets of $^6H_{5/2}$, $^6H_{7/2}$, $^6H_{9/2}$, and $^6H_{11/2}$, respectively. Such sharp and well resolved emission lines of Sm^{3+} ions under indirect excitation indicate the existence of ZnO-to-Sm^{3+} ET that was not reported in Sm^{3+}-doped bulk or nanocrystalline ZnO previously. Besides the characteristic emission lines of Sm^{3+} ions, a broad orange band with a maximum at ~600 nm is also presented in Fig. 3a, which may be associated with the defects such as oxygen interstitials in ZnO nanocrystals[9,11,15] and to some extent limits the ET efficiency between ZnO host and Sm^{3+} ions. The 10 K excitation spectrum for Sm^{3+}-doped ZnO nanocrystals (Fig. 3b), by monitoring the $^4G_{5/2} \rightarrow {}^6H_{9/2}$

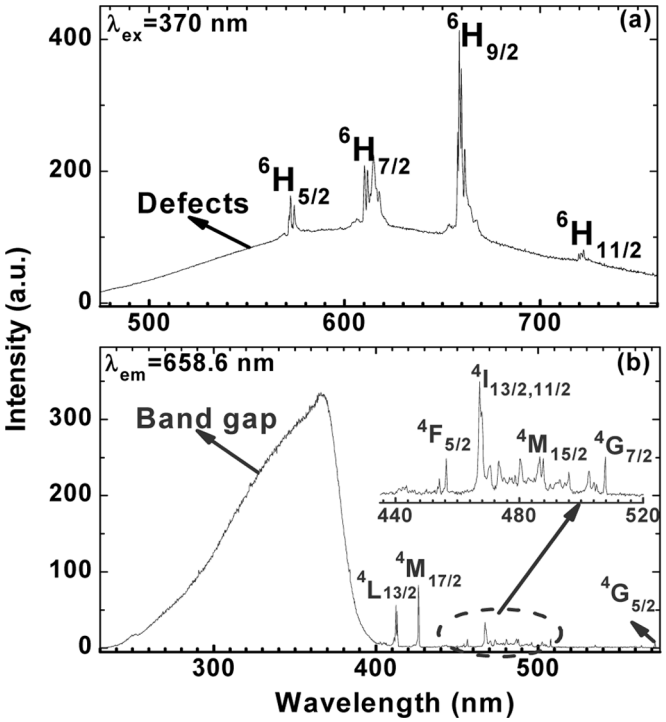

FIGURE 3 The 10 K PL emission (a) and excitation (b) spectra for Sm^{3+} ions doped ZnO nanocrystals.

emission of Sm^{3+} at 658.6 nm, is dominated by an intense broad band centered at ~370 nm, which is attributed to the near-band-edge excitation peak and defects of ZnO nanocrystals[9,28] and close to the band-gap energy (E_g) derived from the RT diffuse reflectance spectrum for Sm^{3+}-doped ZnO nanocrystals. Similar broad excitation band was also observed in Eu^{3+}-doped ZnO nanocrystals[9,14] and ZnO thin films[29] fabricated by the electrodeposition method. This result further confirms that the emissions of Sm^{3+} can be achieved by virtue of an efficient ET process from ZnO to Sm^{3+}. In this process, the hexagonal wurtzite ZnO nanocrystals may act as an effective light-harvesting antenna to absorb UV excitation light and subsequently transfer energy to Sm^{3+} ions, and thereby result in the typical luminescence of Sm^{3+}. Apart from the broad band related to ZnO near-band-edge excitation peak, very sharp and resolved excitation lines from *f-f* transitions of Sm^{3+} ions are also detected in the 10 K excitation spectrum, which are identified and labeled in Figure 3b. These excitation lines with well resolved CF splittings indicate the highly ordered crystalline surroundings around Sm^{3+} ions in ZnO nanocrystals. Moreover, as shown in Figure 3b, the direct excitation lines of Sm^{3+} ions are much weaker than that of ZnO band-gap excitation due to the low absorptions of parity-forbidden *f-f* transitions of Ln^{3+} ions. The above finding establishes that the host sensitized emission is a much more efficient path than the direct excitation of Sm^{3+} in ZnO nanocrystals at low temperature.

Because of different chemical properties between Sm^{3+} and Zn^{2+} ions, multiple sites are expected in Sm^{3+}-doped ZnO nanocrystals similar to the case of Eu^{3+} ion-doped ZnO nanomaterials[8,14] and nanosheet-based ZnO microspheres.[11] To verify the multiple-site structure of Sm^{3+} ions in ZnO nanocrystals, site-selective emission spectrum of Sm^{3+} was measured upon excitation from the ground state $^6H_{5/2}$ to the $^4L_{13/2}$ state of Sm^{3+} at 413.3 nm at 10 K (Fig. 4a). For comparison, the 10 K emission spectrum (560 to 680 nm) of Sm^{3+}-doped ZnO nanocrystals under indirect excitation is also presented in Figure 4b. As shown in Figure 4a, under the site-selective excitation at 413.3 nm, typical emission lines originating from the transitions of $^4G_{5/2} \rightarrow {}^6H_J$ ($J = 2/5$, 7/2 and 9/2) can be observed with the dominant emission line centered at 659.8 nm. Because of Kramers degeneracy for $4f^5$ configuration of Sm^{3+}, the 10 K emission pattern should consist of 3, 4, and 5 emission lines for $^4G_{5/2} \rightarrow {}^6H_J$ ($J = 2/5$, 7/2 and 9/2) transitions when Sm^{3+} ions occupy single lattice site with low-symmetry in ZnO nanocrystals. As a matter of fact, 2, 3, and 3 emission lines for $^4G_{5/2} \rightarrow {}^6H_J$ ($J = 2/5$, 7/2 and 9/2) transitions can be clearly identified when selectively excited at

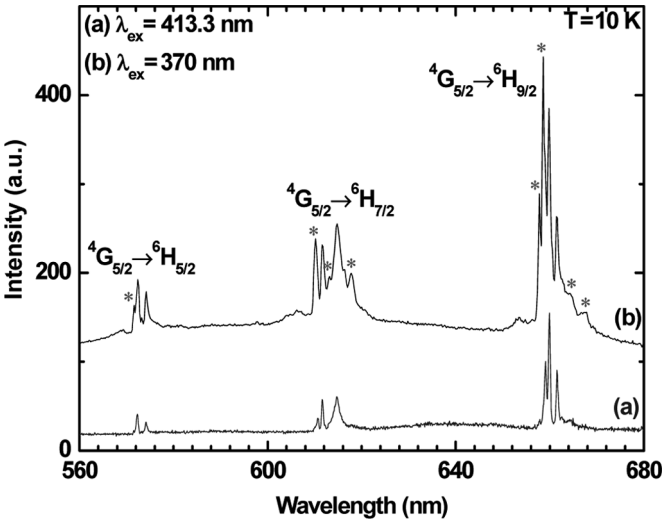

FIGURE 4 The 10 K PL spectra for Sm^{3+} ions doped ZnO nanocrystals under (a) direct and (b) indirect excitation.

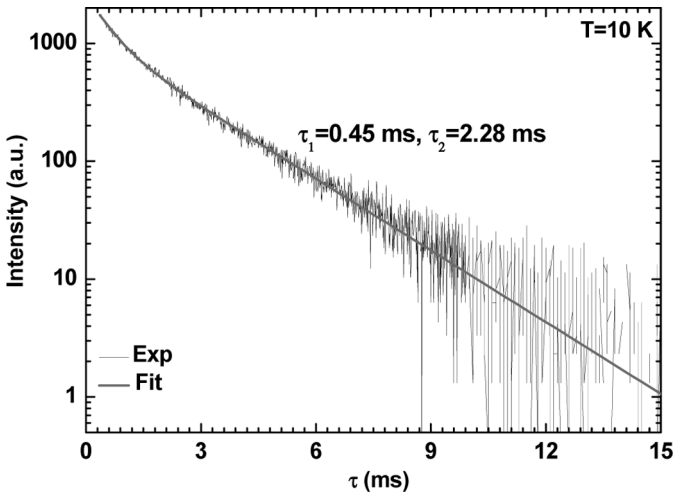

FIGURE 5 The 10 K luminescence decay of Sm^{3+} by monitoring the $^4G_{5/2} \rightarrow {}^6H_{9/2}$ transition at 659.8 nm when excited at 413.3 nm.

413.3 nm, less than theoretically predicted numbers of splitting, suggesting that these emission lines should arise from the single site of Sm^{3+} ions in ZnO nanocrystals. Different from the emission pattern under direct excitation at 413.3 nm, multiple site emissions are detected upon excitation above the ZnO band-gap energy at ~370 nm. Several new emission lines (as marked with star symbols in Figure 4b), with the most intense emission line at 658.6 nm, are found located very close to those lines identified under the direct *f-f* excitation, indicative of a totally different CF environment around Sm^{3+} ions in ZnO nanocrystals (i.e., multiple sites of Sm^{3+} ions in ZnO nanocrystals). The 413.3 nm excitation, which is resonant with the $^6H_{5/2} \rightarrow {}^4L_{13/2}$ transition of Sm^{3+}, can selectively excite specific Sm^{3+} ions in the lattice of ZnO nanocrystals, whereas the 370 nm-excited emission pattern is the superposition of all emissions from various subsets of Sm^{3+} ions in ZnO nanocrystals. As a result, multiple-site emissions of Sm^{3+} ions are detected in Fig. 4b above the band-gap excitation. To gain more insights into the optical properties of multiple sites in ZnO:Sm^{3+} nanocrystals, the luminescence decay of Sm^{3+} was measured at 10 K. The decay curve of $^4G_{5/2}$ shows clearly multi-exponential nature under the 413.3 nm excitation (Fig. 5), by fitting with a double-exponential function, the intrinsic PL lifetime of Sm^{3+} at 659.8 nm is determined to be 0.45 (20%) and 2.28 (80%) ms for the fast and slow components, respectively. Such multi-exponential decay behaviors are understandable due to the overlapping of different decays from multiple Sm^{3+} sites in ZnO nanocrystals, as observed in Nd^{3+} and Tm^{3+} ion-doped ZnO nanocrystals.[5] Unfortunately, owing to the very close CF levels for various subsets of Sm^{3+} ions in ZnO nanocrystals, currently it is difficult to obtain pure luminescence decay curve from single Sm^{3+} site even selectively excited at 413.3 nm.

Like Sm^{3+}-doped ZnO nanocrystals, such multiple-site structure as well as host sensitized PL can be also found in Dy^{3+} ions doped ZnO nanocrystals. As illustrated in Fig. 6a and 6c, characteristic and sharp emission lines of Dy^{3+} ions superimposed on the ZnO defect related emission band are detected upon excitation above the band-gap at ~365 nm at 10 K. The emission lines centered at 580 nm is ascribed to the de-excitation from $^4F_{9/2}$ to its lower multiplet of $^6H_{13/2}$ of Dy^{3+}, implying that the Dy^{3+} emission is related to the nonradiative ET process from ZnO to Dy^{3+}. Such emission lines from the $^4F_{9/2} \rightarrow {}^6H_{13/2}$ transition of Dy^{3+} can also be detected upon direct excitation at 451 nm (Figure 6c). In contrast, the emission pattern upon band-gap excitation is apparently distinct from that under direct excitation at 451 nm. Two new emission lines marked with pound signs appear in addition to the line observed under the direct excitation, which may arise from Dy^{3+} ions located at different CF environments in ZnO nanocrystals. Different luminescence patterns under indirect or direct excitations suggest inhomogeneous CF surroundings for the doped Dy^{3+} ions, thereby confirming the existence of multiple luminescence centers of Dy^{3+} in ZnO nanocrystals. The 10 K excitation spectrum by monitoring the $^4F_{9/2} \rightarrow {}^6H_{13/2}$ transition at 580 nm

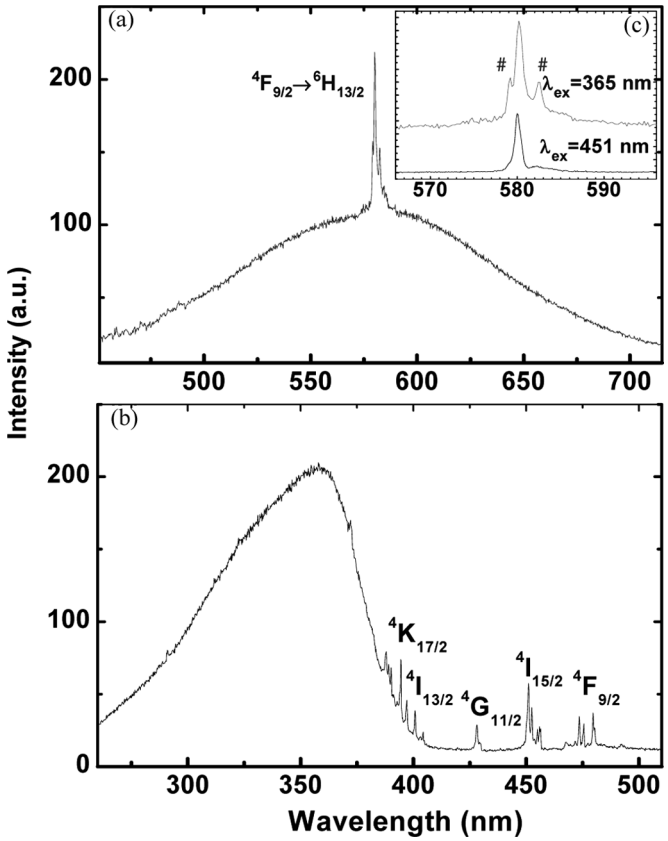

FIGURE 6 The 10 K PL (a) and PL excitation (b) spectra for Dy^{3+} ion-doped ZnO nanocrystals. The inset (c) compares the 10 K PL spectra for Dy^{3+}-doped ZnO nanocrystals under different excitation paths.

exhibits a dominant broad band at ~365 nm (Fig. 6b), which is attributed to the band-gap absorption of ZnO nanocrystals. Similar to the case of Sm^{3+}-doped ZnO nanocrystals, much weaker excitation lines originating from Dy^{3+} ions are observed due to the parity-forbidden nature of *f-f* transitions (Figure 6b). The luminescence decay from $^4F_{9/2}$ of Dy^{3+} also exhibits multi-exponential characteristics (not shown) under the 451 nm excitation, and the intrinsic PL lifetime of $^4F_{9/2}$ can be determined to be 0.83 (70%) and 0.21 (30%) ms by a double-exponential fit.

In summary, Sm^{3+} and Dy^{3+} ions were effectively incorporated into hexagonal wurtzite ZnO nanocrystals by using a sol-gel method, which thus resulted in sharp and typical emission lines of *f-f* transitions. The optical properties of Sm^{3+} and Dy^{3+} ions in ZnO nanocrystals were investigated in detail by means of low temperature steady-state luminescence spectroscopy. Multiple sites of Sm^{3+} and Dy^{3+} ions in ZnO nanocrystals were well identified based on the 10 K PL spectra under different excitation paths. Intense host-sensitized PL of Sm^{3+} or Dy^{3+} ions were achieved upon excitation above the ZnO band-gap. These findings might be of particular interest for further material applications in optoelectronic devices, flat-panel displays, and biological labels.

ACKNOWLEDGMENTS

This work is supported by the One Hundred Talents and Knowledge Innovation Programs of CAS for Key Topics (No. KJCX2-YW-358), NSFC (No. 10774143 and 10974200), the 973 program (No. 2007CB936703), the National High-Tech R&D Program of China (863 Program) (No. 2009AA03Z430), Fujian Provincial Science Fund for Distinguished Young Scholars (No. 2009J06030), and the Key Project of Science and Technology of Fujian Province (No. 2007I0024).

REFERENCES

1. Wang, F.; Liu, X. G. Recent advances in the chemistry of lanthanide-doped upconversion nanocrystals. *Chem. Soc. Rev.* **2009**, *38*, 976–989.

2. Wang, F.; Xue, X. J.; Liu, X. G. Multicolor tuning of (Ln, P)-doped YVO_4 nanoparticles by single-wavelength excitation. *Angew. Chem., Int. Ed.* **2008**, *47*, 906–909.
3. Wang, F.; Liu, X. G. Upconversion multicolor fine-tuning: Visible to near-infrared emission from lanthanide-doped $NaYF_4$ nanoparticles. *J. Am. Chem. Soc.* **2008**, *130*, 5642–5643.
4. Luo, W. Q.; Li, R. F.; Chen, X. Y. Host-sensitized luminescence of Nd^{3+} and Sm^{3+} ions incorporated in anatase titania nanocrystals. *J. Phys. Chem. C.* **2009**, *113*, 8772–8777.
5. Liu, Y. S.; Luo, W. Q.; Li, R. F.; Zhu, H. M.; Chen, X. Y. Near-infrared luminescence of Nd^{3+} and Tm^{3+} ions doped ZnO nanocrystals. *Opt. Express.* **2009**, *17*, 9748–9753.
6. Tachikawa, T.; Ishigaki, T.; Li, J.-G.; Fujitsuka, M.; Majima, T. Defect-mediated photoluminescence dynamics of Eu^{3+}-doped TiO_2 nanocrystals revealed at the single-particle or single-aggregate level. *Angew. Chem. Int. Ed.* **2008**, *47*, 5348–5352.
7. Chen, L.; Zhang, J. H.; Zhang, X. M.; Liu, F.; Wang, X. J. Optical properties of trivalent europium doped ZnO:Zn phosphor under indirect excitation of near-UV light. *Opt. Express.* **2008**, *16*, 11795–11801.
8. Tanner, P. A.; Yu, L. X. Photoluminescence of ZnO:Eu^{3+} nanoflowers. *J. Nanosci. Nanotechnol.* **2008**, *8*, 1307–1311.
9. Liu, Y. S.; Luo, W. Q.; Li, R. F.; Liu, G. K.; Antonio, M. R.; Chen, X. Y. Optical spectroscopy of Eu^{3+} doped ZnO nanocrystals. *J. Phys. Chem. C.* **2008**, *112*, 686–694.
10. Armelao, L.; Bottaro, G.; Pascolini, M.; Sessolo, M.; Tondello, E.; Bettinelli, M.; Speghini, A. Structure-luminescence correlations in europium-doped sol-gel ZnO nanopowders. *J. Phys. Chem. C.* **2008**, *112*, 4049–4054.
11. Zeng, X. Y.; Yuan, J. L.; Wang, Z. Y.; Zhang, L. Nanosheet-based microspheres of Eu^{3+}-doped ZnO with efficient energy transfer from ZnO to Eu^{3+} at room temperature. *Adv. Mater.* **2007**, *19*, 4510–4514.
12. Wang, X.; Kong, X.; Yu, Y.; Sun, Y.; Zhang, H. Effect of annealing on upconversion luminescence of ZnO:Er^{3+} nanocrystals and high thermal sensitivity. *J. Phys. Chem. C.* **2007**, *111*, 15119–15124.
13. Peres, M.; Cruz, A.; Pereira, S.; Correia, M. R.; Soares, M. J.; Neves, A.; Carmo, M. C.; Monteiro, T.; Pereira, A. S.; Martins, M. A.; Trindade, T.; Alves, E.; Nobre, S. S.; Ferreira, R. A. S. Optical studies of ZnO nanocrystals doped with Eu^{3+} ions. *Appl. Phys. A.* **2007**, *88*, 129–133.
14. Liu, Y. S.; Luo, W. Q.; Li, R. F.; Chen, X. Y. Spectroscopic evidence of the multiple-site structure of Eu^{3+} ions incorporated in ZnO nanocrystals. *Opt. Lett.* **2007**, *32*, 566–568.
15. Zeng, X. Y.; Yuan, J. L.; Zhang, L. Synthesis and photoluminescent properties of rare earth doped ZnO hierarchical microspheres. *J. Phys. Chem. C.* **2008**, *112*, 3503–3508.
16. Wang, J.; Zhou, M. J.; Hark, S. K.; Li, Q.; Tang, D.; Chu, M. W.; Chen, C. H. Local electronic structure and luminescence properties of Er doped ZnO nanowires. *Appl. Phys. Lett.* **2006**, *89*, 221917.
17. Pereira, A. S.; Peres, M.; Soares, M. J.; Alves, E.; Neves, A.; Monteiro, T.; Trindade, T. Synthesis, surface modification and optical properties of Tb^{3+}-doped ZnO nanocrystals. *Nanotechnology.* **2006**, *17*, 834–839.
18. Luo, W. Q.; Li, R. F.; Liu, G. K.; Antonio, M. R.; Chen, X. Y. Evidence of trivalent europium incorporated in anatase TiO_2 nanocrystals with multiple sites. *J. Phys. Chem. C.* **2008**, *112*, 10370–10377.
19. Chengelis, D. A.; Yingling, A. M.; Badger, P. D.; Shade, C. M.; Petoud, S. Incorporating lanthanide cations with cadmium selenide nanocrystals: A strategy to sensitize and protect Tb(III). *J. Am. Chem. Soc.* **2005**, *127*, 16752–16753.
20. Frindell, K. L.; Bartl, M. H.; Popitsch, A.; Stucky, G. D. Sensitized luminescence of trivalent europium by three-dimensionally arranged anatase nanocrystals in mesostructured titania thin films. *Angew. Chem. Int. Ed.* **2002**, *41*, 960–962.
21. Li, L.; Tsung, C. K.; Yang, Z.; Stucky, G. D.; Sun, L. D.; Wang, J. F.; Yan, C. H. Rare-earth-doped nanocrystalline titania microspheres emitting luminescence via energy transfer. *Adv. Mater.* **2008**, *20*, 903–908.
22. Kim, S.; Rhee, S. J.; Li, X.; Coleman, J. J.; Bishop, S. G. Photoluminescence and photoluminescence excitation spectroscopy of multiple Nd^{3+} sites in Nd-implanted GaN. *Phys. Rev. B.* **1998**, *57*, 14588–14591.
23. Cheng, B. M.; Yu, L. X.; Duan, C. K.; Wang, H. S.; Tanner, P. A. Vacuum ultraviolet and visible spectra of ZnO:Eu^{3+} prepared by combustion synthesis. *J. Phys-Condens Mat.* **2008**, *20*, 345231.
24. Ishizumi, A.; Kanemitsu, Y. Structural and luminescence properties of Eu-doped ZnO nanorods fabricated by a microemulsion method. *App. Phys. Lett.* **2005**, *86*, 253106.
25. Du, Y. P.; Zhang, Y. W.; Sun, L. D.; Yan, C. H. Efficient energy transfer in monodisperse Eu-doped ZnO nanocrystals synthesized from metal acetylacetonates in high-boiling solvents. *J. Phys. Chem. C.* **2008**, *112*, 12234–12241.
26. Kortum, G. *Reflectance Spectroscopy*; Springer-Verlag: New York, 1969.
27. Cao, G.; Rabenberg, L. K.; Nunn, C. M.; Mallouk, T. E. Formation of quantum-size semiconductor particles in a layered metal phosphonate host lattice. *Chem. Mater.* **1991**, *3*, 149–156.
28. Lima, S. A. M.; Sigoli, F. A.; Davolos, M. R.; Jafelicci, M. Europium(III)-containing zinc oxide from Pechini method. *J. Alloys Compd.* **2002**, *344*, 280–284.
29. Pauporte, T.; Pelle, F.; Viana, B.; Aschehoug, P. Luminescence of nanostructured Eu^{3+}/ZnO mixed films prepared by electrodeposition. *J. Phys. Chem. C.* **2007**, *111*, 15427–15432.